Supplementary Material: Figure Legends and Methods

Supplementary Figure Legends

Supplementary Figure 1. Identification of NHP CD4+ T_{SCM} in healthy macaques. (**A)** Flow cytometric analysis of PBMC from a healthy rhesus macaque (RM). Plots show live CD3+CD4+CD8- lymphocytes. **(B)** Mean±SEM percent of T_N, T_{SCM}, T_{CM} and T_{EM} among CD4+ T-cells in the peripheral blood (PB) of RM (n=6). **(C)** as in **B** but in different organs. Data indicate the proportion relative to PB (dashed bar). Data in **B** and **C** are expressed on a log scale. MLN: mesenteric lymph node (LN); ALN: axillary LN; ILN: inguinal LN; Spl: spleen; BM: bone marrow; Jej: jejunum. **(D)** Percent of CD4+ T-cell subsets expressing CCR5, IL-18Rα, CD38, Ki-67, HLA-DR or CXCR3. CD130 (IL-6st) and CD122 are indicated as mean fluorescence intensity (MFI). * = $p < 0.05$ vs. T_{SCM}.

Supplementary Figure 2. CD8+ T_{SCM} are LFA-1^{hi} and proliferate as conventional memory cells in peripheral tissues. (A) Representative flow cytometric analysis of LFA-1 expression by splenic T_N, T_{SCM}, T_{CM} and T_{EM}. **(B)** MFI of LFA-1 by the same T-cell subsets from 5 different animals. **(C)** Percent Ki-67+ T-cell subsets isolated from the LN (n=8), the spleen (n=5) and the BM (n=5). Boxes in **B** and **C** show the interquartile range and median values. **D)** Flow cytometric analysis of BrdU incorporation *in vivo* by pigtail macaque CD8+ T-cell subsets before and at day 21 post-infection (p.i.) with $SIV_{mac}239$. Numbers indicate the percentage of BrdU+Ki67+ cells. Similar data were obtained from a second animal.

Supplementary Fig. 3. Identification and dynamics of SIV-specific CD8+ T-cells in vivo. (A) Representative tetramer staining of CM9- and TL8-specific CD8+ T-cells in a RM before and at day 120 after infection with $SIV_{mac}251$. Plots are gated on live CD3+CD8+CD4- lymphocytes. Numbers indicate the percentage of tetramer+ cells. **(B)** Expression of Ki-67,

HLA-DR and CD38 on TL8+ CD8+ T-cells (blue) superimposed to total CD8+ T-cells (grey) at day 14 and day 70 p.i. with $SIV_{mac}251$. Numbers indicate the percent of cells identified by the quadrants. **(C)** Percent of SIV-specific CD8+ T-cells at different time points following infection as in **A.** The interquartile range and the median are shown. **(D)** Absolute count of CM9- and TL8-specific T_{SCM}, T_{CM} and T_{EM} in the PB at different days p.i. (mean±SEM of 6 animals). Data in **C** and **D** are expressed in log scale.

Supplementary Figure 4. Antigen-specific T_{SCM} maintain self-renewal and multipotent capacity in chronic infection. (A) Polyclonal CD8+ T-cell subsets were sorted on the basis of CD45RA, CCR7, CD28 and CD95 expression, labeled with CFSE and stimulated with autologous antigen-presenting cells pulsed with CM9 and TL8 peptides for 6 days. SIV-specific T-cells (CM9: red; TL8: blue) were detected with fluorescently-conjugated pMamuA*01 tetramers. Polyclonal CD8+ T-cells define the fluorescence of unstimulated cells. SIV-specific CD8+ T-cells in the T_N population were not present and, thus, not depicted (N/A). **(B)** CD45RA and CCR7 expression by CM9- and TL8-specific CD8+ T-cells that diluted CFSE overlayed on top of polyclonal CD8+ T-cell subsets (grey). Numbers indicate the percentage of cells inside each quadrant.

Supplementary Figure 5. Stable differentiation and localization of SIV-specific T_{SCM} during chronic infection. (A) Pie charts depicting the proportion of CM9- and TL8-specific CD8+ T-cells with different phenotypes (T_{SCM}: CD45RA+CCR7+CD27+CD95+; T_{CM}: CD45RA-CCR7+; T_{EM}: CD45RA-CCR7-; T_{TE} (terminal effectors): CD45RA+CCR7- at day >335 p.i.; **(B)** Frequency of CM9- and TL8-specific CD8+ T-cell subsets (log scale) in the ILN from 2 animals at different days post SIV infection. **(C)** Distribution of CM9- and TL8-specific T-cell subsets in multiple organs during chronic SIV infection. PB: peripheral blood; MLN:

mesenteric lymph node (LN); ALN: axillary LN; ILN: inguinal LN; Spl: spleen; BM: bone marrow.

Supplementary Figure 6. (A) Annexin V expression by antigen-specific T-cell subsets from chronically SIV-infected animals after culture in the presence of aCD28 and aCD49d antibodies for 40 hours. Left panel: identification of antigen-specific cells by tetramer staining of ViViD-CD3+CD8+CD4- cells. Right panel: T_{SCM} were defined as CD45RA+CCR7+CD95+, T_{CM} as CD45RA-CCR7+ and T_{EM} as CD45RA-CCR7-. **(D)** Summary of annexin V expression in CM9- and TL8-specific CD8+ T-cell subsets identified as in **C** (n=7). Boxes show the interquartile range and median values. * = $p < 0.05$.

Supplementary Figure 7. Flow cytometry sorting strategy for the isolation of CD8+ T-cell subsets. (A) CD8+ T-cells were enriched via magnetic negative selection and subsequently stained with ViViD and surface monoclonal antibodies to CD3, CD4, CD8, CD45RA, CCR7, CD28 and CD95. CD8+ live-gated T-cells were sorted as follows: a first gate was drawn to identify "resting" ($FSC^{low}SSC^{low}$) and "blasting" ($FSC^{hi}SSC^{hi}$) cells; "resting" and "blasting" cells were subsequently sorted in T_N (CD45RA+CCR7+CD28+CD95-), T_{SCM} (CD45RA+CCR7+CD28+CD95+), T_{CM} (CD45RA-CCR7+) and T_{EM} (CD45RA-CCR7-) cells. **(B)** Percent of HLA-DR+ cells in "blasting" CD8+ T-cell subsets. **(C)** Number of *LEF1*, *BCL2* and *MCL1* mRNA copies (log scale) in "resting" and "blasting" CD8+ T-cell subsets. * = $p < 0.05$, + = $p < 0.01$, # = $p < 0.001$; Student's t-test for repeated measures.

Supplementary Methods

Animals. Indian rhesus or pigtailed macaques, either uninfected or infected with $SIV_{mac}239$ or $SIV_{mac}251$, were used for this study.

Three Mamu-A*01+ rhesus macaques (housed at ABL Laboratories, Rockville MD) were immunized at 0 and 8 weeks with intramuscular (i.m.; 3 mg) and intradermal (1 mg) inoculations of DNA-SIVgpe at week 21, 40 and 57/61, then boosted with ALVAC-SIVgpe. Each vaccination with ALVAC-SIVgpe boost consisted of 10^8 PFU in 150 µL of PBS delivered intramuscularly. At week 40 and 57/61 all animals also received the homologous gp120 protein, adjuvanted in Alum, which was administered intramuscularly in the opposite thigh to the ALVAC-SIVgpe or control inoculum; three animals received Alum alone as a control. Infectious challenge was conducted with a single high dose (TCID50: 6,100) of $SIV_{mac}251$, given intrarectally 4 weeks after the last immunization (Vaccari *et al*., manuscript in preparation).

Four Mamu-A*01+ rhesus macaques (housed at Bioqual Inc., Rockville, MD) received adoptive cell transfer of SIV-specific CD8+ T-cell clones either 1 day before or 3 days after i.v. infection with 100 AID50 $SIV_{mac}251$ (1). Two of these animals received subcutaneous (s.c.) low-dose (10^4 U/Kg/d) IL-2 injections daily for 10 days following adoptive cells transfer. Transferred antigen-specific T-cells were demonstrated to be undetectable by day 3 post transfer in the peripheral blood and in multiple body sites at all time points (1). These treatments did not influence the generation or frequency of endogenous SIV-specific T-cell responses compared to naïve, untreated animals. Naïve and cell recipient animals are shown in Fig. 3A-D, Supplementary Fig. 4, 6; naïve and vaccinated animals in Fig. 3C-F.

Four Mamu-A*01+ rhesus macaques (housed at the Oregon National Primate Research Center according to the standards of the Animal Care and Use Committee and the NIH Guide for the Care and Use of Laboratory Animals) were vaccinated three times i.m. with $SIV_{mac}239$ Env-Gag-Pol-Vif DNA prime in both arms and both thighs; each vaccination was separated by a period of 4 weeks. Animals were boosted 12 weeks later with Merck Ad5 containing $SIV_{mac}239$ Env-Gag-Pol-Vif. Three unvaccinated animals were used as controls. All animals were infected with low dose (TCID50 100 or 300) $SIV_{mac}239$, given intrarectally at 28-32 weeks post-boost. These animals were used to generate Supplementary Fig. 5A, B.

Pigtail macaques were housed at the NIH animal center, Poolesville, MD.

None of the treatments described above significantly altered the course of SIV infection or viral dynamics.

Viral RNA in plasma was measured as described (2).

Isolation of cells from blood and tissues. Mononuclear cells from the peripheral blood (PBMC), the bronchoalveolar lavage and tissues were isolated as described previously (3). Either fresh or frozen cells were used for immunophenotyping and functional assays, as specified in the text. PBMC were frozen in fetal bovine serum containing 10% DMSO and stored in liquid phase nitrogen until analysis.

Antibodies, Mamu-A*01 tetramers and flow cytometry. Conjugated monoclonal antibodies were purchased from a variety of vendors; in some cases, purified monoclonal antibodies were conjugated in our laboratory (http://www.drmr.com/abcon). Dead cells were excluded in all assays by using a Violet Viability Dye (Life Technologies). Recombinant Mamu-A*01 pMHCI tetramers, presenting the Tat TL8 (TTPESANL; residues 28–35) or Gag CM9 (CTPYDINQM; residues 181–189) peptides were produced as described previously (4). The $SIV_{mac}239$- and $SIV_{mac}251$-encoded Tat epitopes, STPESANL (SL8) and TTPESANL (TL8),

respectively, are both recognized by TL8-specific T-cells; throughout the manuscript we refer to either response as TL8-specific. Flow cytometric data were compensated and analyzed with FlowJo software (Treestar, Inc.). Data were formatted with Pestle software and presented with SPICE software (5).

Gene expression analysis of sorted T-cells. Briefly, PBMC from 5 healthy and 4 chronically SIV-infected animals were thawed in complete medium containing benzonase (EMD Chemicals) and washed extensively; CD8+ T-cells were then magnetically sorted by negative depletion (Miltenyi Biotech). Enriched cells were stained with surface monoclonal antibodies to identify T-cell subsets and subsequently sorted by flow cytometry. Fifty polyclonal CD8+ T-cells (either "resting" or "blasting", sorted in triplicate) were sorted by flow cytometry into a 96-well plate for assay in a Fluidigm BioMark single-cell qPCR system. Preliminary experiments demonstrated that gene expression averaged over 100 single cell wells was nearly identical to that observed when 100 cells were sorted in bulk into a single well. Moreover, results from replicate bulk sorts were highly reproducible (<10% CV). Thus, the adaptation of this single-cell system to relatively small numbers of cells sorted in bulk is feasible.

The Fluidigm BioMark qPCR was performed as follows. First, mRNA targets were chosen based on their known or suspected relevance to T-cell differentiation and function. TaqMan primers/probes were then purchased (Life Technologies) for these targets. Second, all primer/probe sets were qualified by the Ct Slope testing method described by the manufacturer (http://www3.appliedbiosystems.com/cms/groups/mcb_marketing/documents/generaldocuments/cms_040377.pdf). Briefly, a dilution series of bulk mRNA (pooled from resting and PHA-stimulated rhesus macaque PBMC) was constructed and assayed on the Fluidigm Biomark chip (described below). Primers/probes were deemed satisfactory if the target

signal was linear across dilutions (R^2>0.99) and if amplification was efficient. Efficiency was examined two ways: (i) first by ensuring that amplicons doubled with every PCR cycle during the log phase, (ii) by plotting and fitting the Ct vs. cDNA concentration (Log10). Primer/probe sets were accepted if the slope of the fit ("efficiency") was -3.3 +/- 10%. Fifteen percent of catalogued TaqMan primers failed these linearity or efficiency tests, and were deemed unsuitable for Fluidigm BioMark analyses; however, in all cases, alternate catalogued primers for a given target were found to be suitable. Third, 96 qualified primers/probes were mixed together and used for reverse transcription/*in vitro* cDNA amplification from sort-purified cells, using the CellsDirect system (Life Technologies). cDNA was amplified for 18 cycles in this step. 96-well plates with cDNA were then stored at -80°C until analysis. Finally, Fluidigm BioMark qPCR was performed on a proprietary chip (Fludigm) with reaction chambers situated at the intersection of microfluidic channels. cDNA from the cellular material was applied to one side of the chip, while Taqman primers/probes for each target were added to wells on the other side. The chip was then loaded into the instrument, which houses an integrated fluidics controller. An aliquot of cDNA from each cell sample and primers/probes for one target were then distributed into each of the 9218 PCR reaction chambers (96 cells X 96 gene targets). Forty cycles of PCR were performed on the chip, and fluorescence from the probes was measured with each cycle. C_t values were recorded for analysis and 40-C_t values were plotted. If less than 50 cells were sorted, Ct values were normalized according to the formula: 40-C_t+Log[50/x], where x is the number of sorted cells.

Supplementary References

1. Bolton DL, et al. Trafficking, persistence, and activation state of adoptively transferred allogeneic and autologous Simian Immunodeficiency Virus-specific CD8(+) T cell clones during acute and chronic infection of rhesus macaques. *J Immunol.* 184(1):303-314.

2. Lugli E, Mueller, YM, Lewis, MG, Villinger, F, Katsikis, PD, and Roederer, M. IL-15 delays suppression and fails to promote immune reconstitution in virally suppressed chronically SIV-infected macaques. *Blood.* 2011; 118(9):2520-2529.

3. Lugli E, et al. Transient and persistent effects of IL-15 on lymphocyte homeostasis in nonhuman primates. *Blood.* 2010; 116(17):3238-3248.

4. Price DA, et al. Avidity for antigen shapes clonal dominance in CD8+ T cell populations specific for persistent DNA viruses. *J Exp Med.* 2005; 202(10):1349-1361.

5. Roederer M, Nozzi, JL, and Nason, MX. SPICE: Exploration and analysis of post-cytometric complex multivariate datasets. *Cytometry A.* 2011; 79(2):167-174.

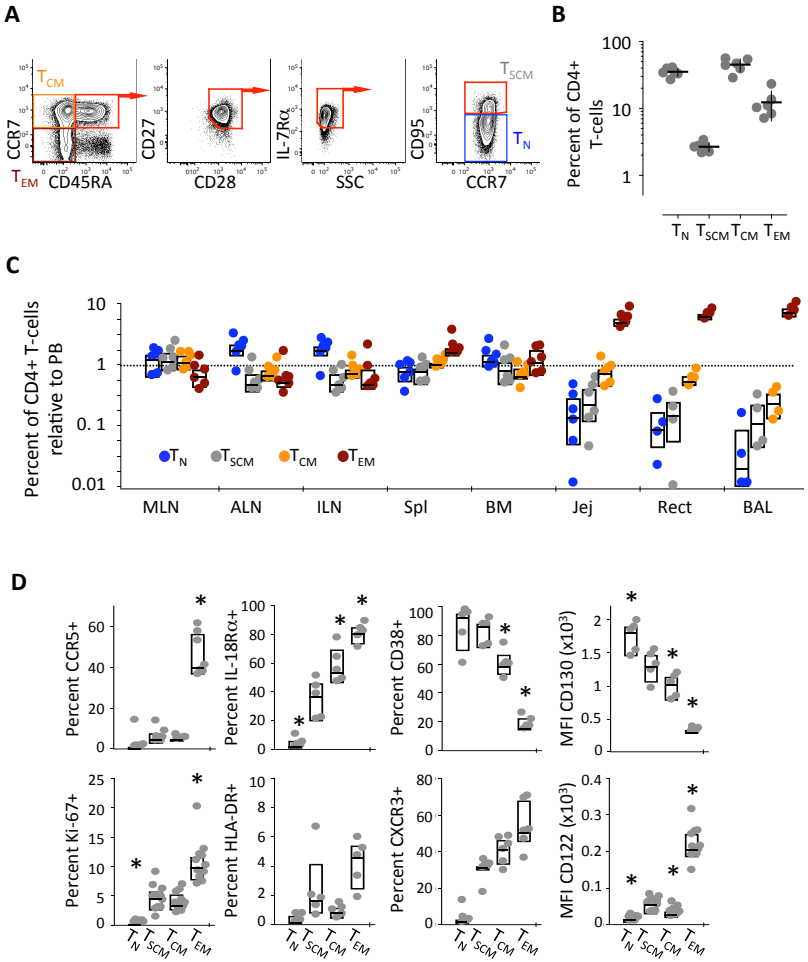

Supplementary Fig. 1

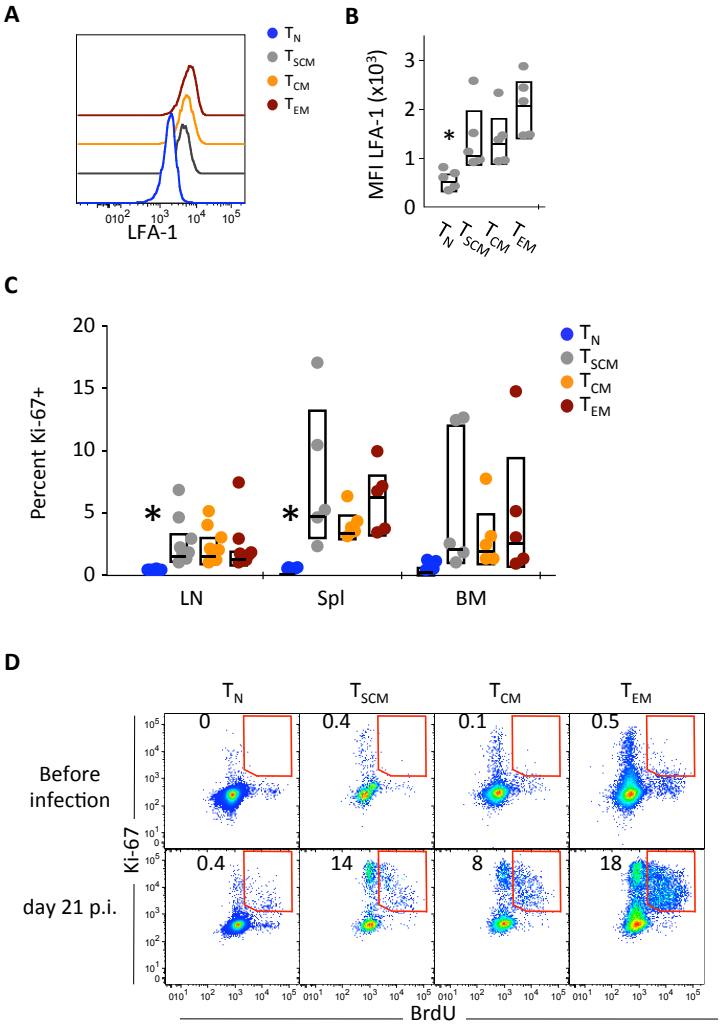

Supplementary Fig. 2

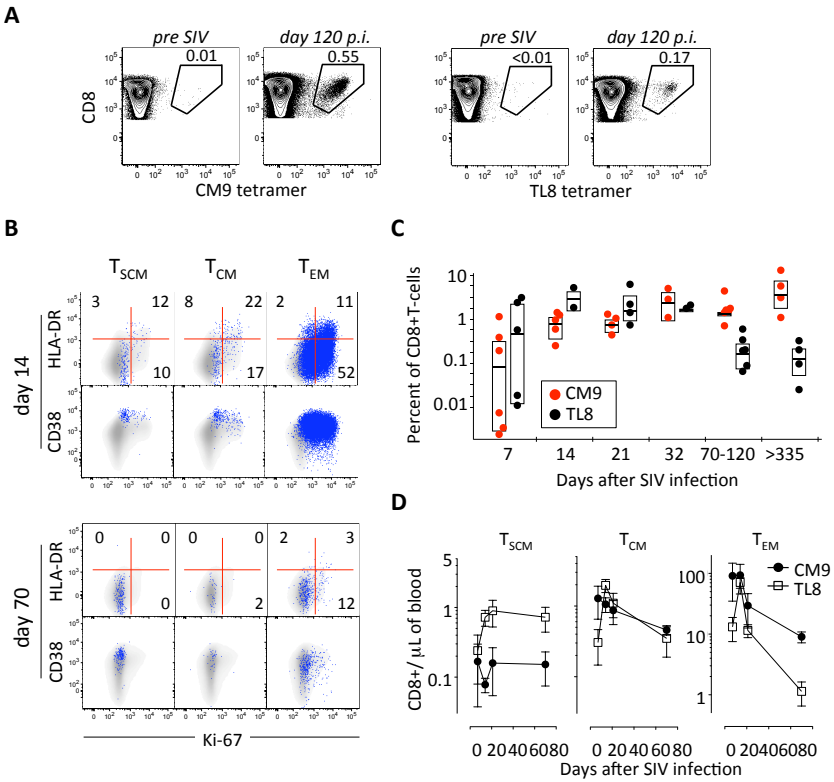

Supplementary Fig. 3

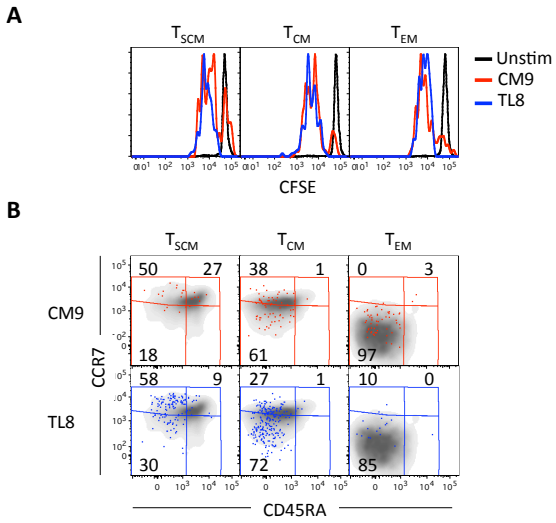

Supplementary Fig. 4

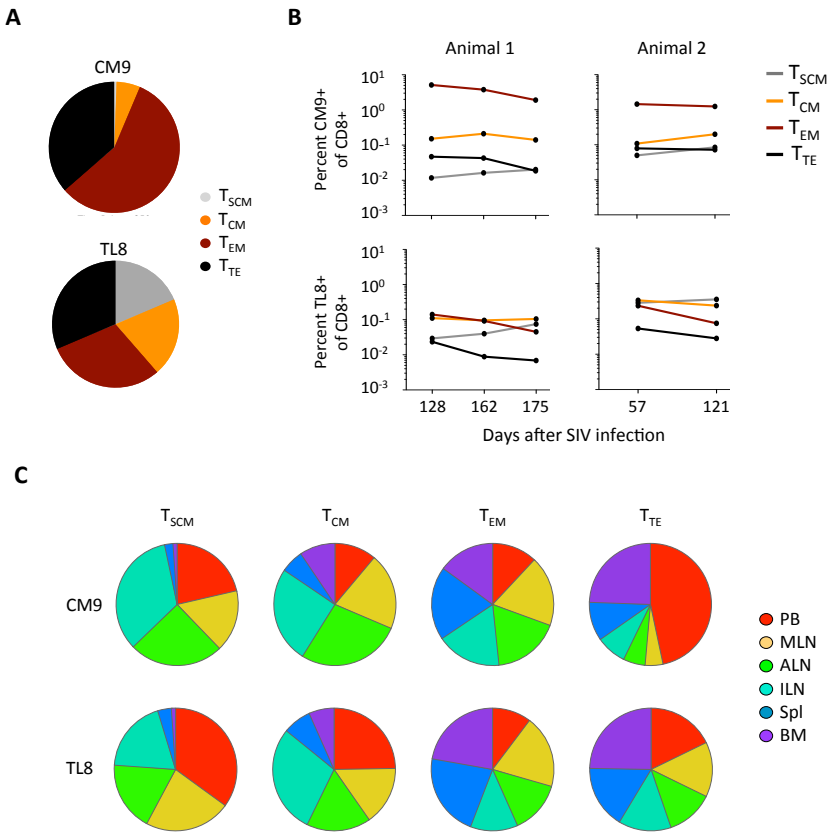

Supplementary Fig. 5

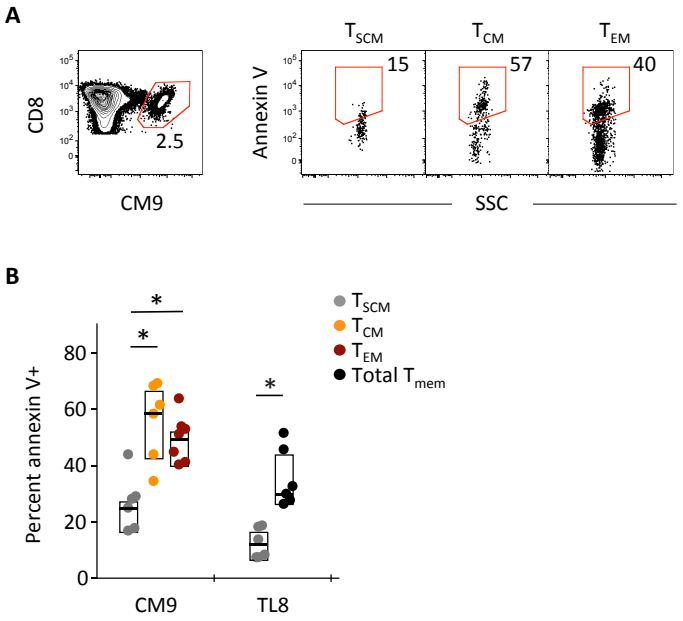

Supplementary Fig. 6

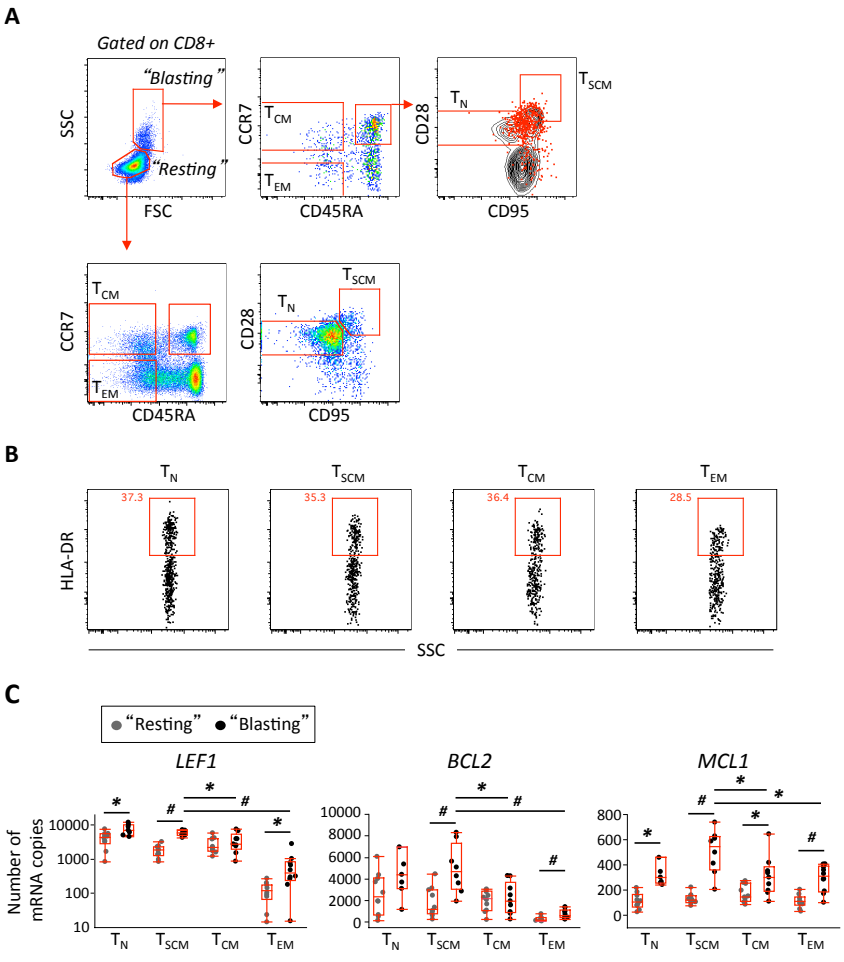

Supplementary Fig. 7